European Journal of Chemistry 5 (2) (2014) 305-310

European Journal of Chemistry

Journal homepage: www.eurjchem.com

Vibrational spectra and normal coordinate analysis of lithium pyruvate monohydrate and its isotopic compounds

Kazuhiko Hanai [a,*], Akio Kuwae [a], Ko-Ki Kunimoto [b] and Soh-Ichi Kitoh [b]

[a] *Graduate School of Natural Sciences, Nagoya City University, Mizuho-Ku, Nagoya 467-8501, Japan*
[b] *Division of Material Sciences, Graduate School of Natural Science and Technology, Kanazawa University, Kakuma-Machi, Kanazawa 920-1129, Japan*

**Corresponding author at: Graduate School of Natural Sciences, Nagoya City University, Mizuho-Ku, Nagoya 467-8501, Japan. Tel.: +81.52.8725856. Fax: +81.52.8725857. E-mail address: hanai@nsc.nagoya-cu.ac.jp (K. Hanai).*

ARTICLE INFORMATION

DOI: 10.5155/eurjchem.5.2.305-310.1004

Received: 18 December 2013
Received in revised form: 31 January 2014
Accepted: 01 February 2014
Online: 30 June 2014

KEYWORDS

Gem-Diol form
Isotope shifts
IR spectroscopy
Raman spectroscopy
Normal coordinate analysis
Lithium pyruvate monohydrate

ABSTRACT

IR and Raman spectra of lithium pyruvate monohydrate and its O- and C-deuterated and ^{13}C- and ^{18}O-substituted compounds have been recorded in the solid state, and the observed bands have been assigned by using the isotope effects and the normal coordinate calculations based on the *gem*-diol structure (lithium 2,2-dihydroxypropionate). The refined force constants have well reproduced the observed frequencies and the ^{13}C- and ^{18}O-shifts. These results support the structures of these compounds discussed by many authors. The potential energy distributions show that many vibrational modes are very complicated except for the well-known group vibrations. The additive property of the isotopic frequency shifts has also been discussed.

1. Introduction

α-Keto acids (pyruvates) are a group of metabolites of biological or biochemical importance. Therefore, their spectral studies have been published by many authors [1-34]. Quantum chemical and conformational studies have also been made [31,32,34-38]. Bellamy *et al.* [3,4] reported the IR spectra of some hydrates including lithium pyruvate hydrate and concluded that these hydrates have *gem*-diol structures in the solid state. Long and George [6,7] came to the same conclusion for this pyruvate from the IR and Raman spectra. However, their assignments for the solid lithium salt are partial, although they carried out the normal coordinate calculation for the keto form, which the pyruvate ion takes in aqueous solution. Sodium 3-fluoropyruvate hydrate was also found to have the diol form by Hurley and his coworker's X-ray analysis and IR and NMR studies [23].

In the previous paper [33], we discussed the structures of lithium pyruvate hydrate (Li-Pyr·H_2O) and sodium pyruvate (Na-Pyr) by the vibrational and ^{13}C NMR spectra in the solid state and in aqueous solution and concluded that the solid lithium salt hydrate has the *gem*-diol structure, namely, is lithium 2,2-dihydroxypropionate, whereas the solid sodium salt takes the ordinary keto form. Zhu *et al.* [34] also reported the results of the solid state ^{17}O NMR measurements for the pyruvates and gave the same conclusion. Thus, the present paper deals with the detailed vibrational assignments based on this structure, using the isotope effects (deuteration; and ^{13}C- and ^{18}O-labelings) and the normal coordinate calculations, and with some relations between the isotope shifts on the ^{13}C- and ^{18}O-labelings. We also attempted to clarify the structure of the solid lithium salt hydrate by X-ray analysis [39]. Although the accurate analysis was not attained owing to the low quality of the single crystals, a rough structure obtained was used for the vibrational calculations.

2. Experimental

2.1. Materials

The samples (Li-Pyr·H_2O and its O-deuterated, 2-C(^{18}OH)$_2$, and ^{13}C-labeled compounds) used in this study are the same as in our previous paper [33]. Li-Pyr·H_2O was prepared also by ion exchange of the sodium salt using cation exchange resin (Amberlite IRC-50 (Li^+ type)). In the O-deuteration process there is the possibility that the H-D exchange reaction between the CH_3 group and D_2O occurs through keto-enol tautomerism to give stepwise-deuterated molecules (those having groups of CH_2D-, CHD_2-, or CD_3-) [22]. However, in our ^1H NMR measurements of D_2O solutions of the lithium and sodium salts, the

ISSN 2153-2249 (Print) / ISSN 2153-2257 (Online)
http://dx.doi.org/10.5155/eurjchem.5.2.305-310.1004

integrated peak intensities hardly vary over a period of several days; these findings indicate that such exchange is negligible. It has also been reported that the sodium salt is unstable in aqueous solution and contaminated with small amounts of the dimer, etc. [40]; judging from the above NMR spectra, these impurities in the samples used are negligibly small in quantity. The 2-$^{13}C(^{18}OH)_2$ analog was prepared from the 2-^{13}C pyruvate by the method reported previously [33].

The CD_3 compound (Li-Pyr-d_3·H_2O) was prepared according to the following processes: (1) acetic acid-d_4 (CEA, 99.4%D) was converted to acetyl-d_3 bromide by phosphorus tribromide [41]; (2) the distilled bromide was allowed to react with cuprous cyanide [42]; (3) the cyanide obtained was distilled and hydrolyzed to pyruvic acid-d_4 by concentrated hydrochloric acid-d (Aldrich, 99%D) [42]; and (4) the distilled acid was passed through Amberlite IRC-50(Li^+) to obtain the lithium salt. The hydrated lithium salt obtained thus was purified by precipitation from an aqueous solution with acetone. Its deuteration purity was checked by NMR spectroscopy. Li-Pyr-d_3·D_2O was prepared by the same method as in the CH_3 compound [33].

2.2. Spectra

IR spectra were obtained on JASCO 403G and PerkinElmer 1640 IR spectrometers, and Perkin Elmer 1720X and Spectrum One FT-IR spectrometers in KBr disks for the hydrates; and in Nujol and H.C.B. (Hexachlorobutadiene) mulls for the deuterates. Raman spectra were recorded on a Perkin Elmer System 2000 FT-Raman spectrometer (Nd:YAG laser: 1064 nm) using the samples sealed in glass capillary tubes. ^1H NMR spectra of D_2O solutions were measured on a JEOL GX-270 spectrometer using DSS as an internal standard.

3. Results and discussion

Figures 1 and 2 show the IR spectra of Li-Pyr·H_2O and its deuterate, and Li-Pyr-d_3·H_2O and its deuterate in the solid state, respectively. The corresponding Raman spectra are shown in Figures 3 and 4. Complicated spectral changes are observed on O-deuteration for the two hydrates. The IR spectral patterns of these hydrates in the 3000 and 1600 cm^{-1} regions are very similar to those of sodium fluoropyruvate hydrate, which has been revealed to have the *gem*-diol structure by X-ray analysis [23]. As discussed for Li-Pyr·H_2O and its deuterate in the previous paper [33], these spectral changes can be explained on the basis of the diol form.

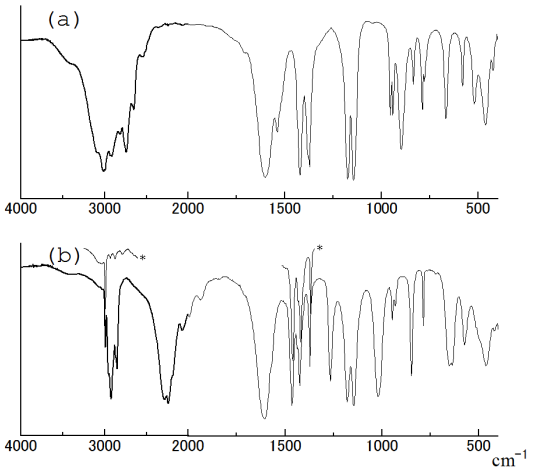

Figure 1. IR spectra of (a) Li-Pyr·H_2O and (b) Li-Pyr·D_2O in the solid state. The spectrum (a) was recorded in a KBr disk and the spectrum (b) in a Nujol mull. The spectra marked with an asterisk are those in an H.C.B. mull. From Hanai, Kuwae, Sugawa, Kunimoto, and Maeda [33] with permission.

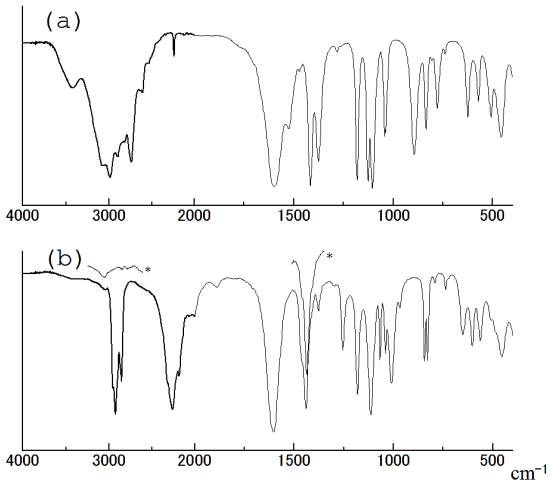

Figure 2. IR spectra of (a) Li-Pyr-d_3 · H_2O and (b) Li-Pyr-d_3 · D_2O in the solid state. The spectrum (a) was recorded in a KBr disk and the spectrum (b) in a Nujol mull. In the former a weak broad band around 3420 cm^{-1} is not observed in a Nujol mull, resulting from moisture in the disk. In the latter the spectra marked with an asterisk are those in an H.B.C. mull.

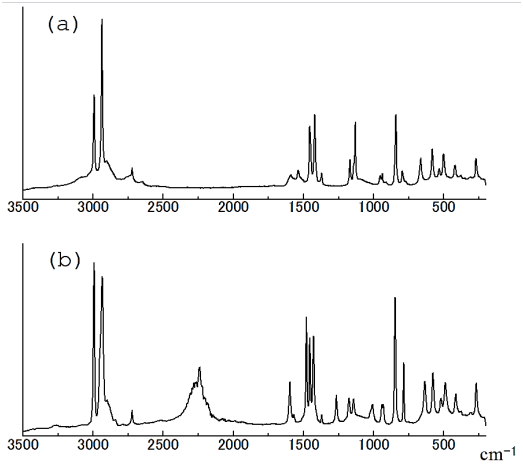

Figure 3. FT-Raman spectra of (a) Li-Pyr·H_2O and (b) Li-Pyr·D_2O in the solid state. From Hanai, Kuwae, Sugawa, Kunimoto, and Maeda [33] with permission.

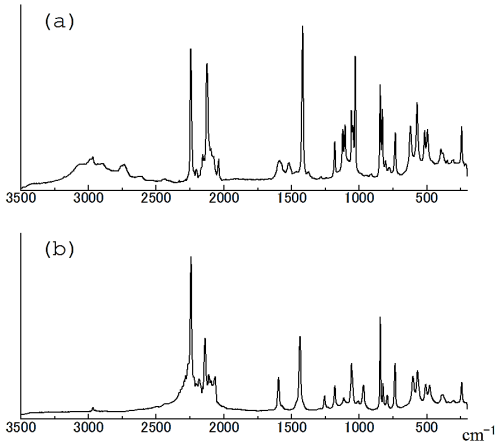

Figure 4. FT-Raman spectra of (a) Li-Pyr-d_3 · H_2O and (b) Li-Pyr-d_3 · D_2O in the solid state.

Table 1. Observed frequencies, isotope shifts (cm^{-1}) [a], and assignments [b] for solid Li-Pyr.H_2O.

IR	$\Delta\nu_a$	$\Delta\nu_b$	$\Delta\nu_c$	$\Delta\nu_d$	$\Delta\nu_e$	$\Delta\nu_f$	$\Delta\nu_g$	Raman	$\Delta\nu_a$	$\Delta\nu_b$	$\Delta\nu_c$	Assignments
A'												
3016.2 vs	-4.7	-9.4	-1.2	-3.3	-18.9	-12.8	-22.2	-	-	-	-	OH str.
2995.7 vw	0.3	0.3	-10.7	-0.2	-1.5	-2.0	-1.7	2992.0 ms	-0.3	-0.4	-10.4	CH_3 asym. str.
2932.7 w	-	0.3	-4.7	-1.6	1.7	-0.2	0.1	2936.6 vs	-0.3	-0.6	-4.5	CH_3 sym. str.
1539.4 m	-	-10.4	-0.4	-4.5	-11.9	-6.0	-16.4	1537.3 w	-5.1	-10.5	-0.4	OH bend + $C_{(1)}C_{(2)}$ str.
-	-	-	-	-	-	-	-	1455.1 ms	-0.7	-1.4	-2.2	CH_3 asym.def.
1420.8 s	-22.8	0.2	-1.5	-1.6	-0.2	-2.0	-1.8	1419.2 ms	-25.5	-0.6	-0.7	CO_2^- sym. str. + OH bend + CO_2^- bend
1372.0 s	-5.0	0.0	-9.0	0.0	-1.0	-1.0	-1.0	1369.9 w	-2.9	-0.7	-10.6	CH_3 sym. def.
1145.0 s	1.0	-21.6	-1.8	-3.0	-20.0	-1.4	-23.0	1140.3 sh	-0.6	-20.2	-4.2	CH_3 rock + $C_{(2)}C_{(3)}$ str. + OCO sym. str.
1134.0 sh	-1.0	-26.0	-6.0	-4.0	-26.0	-4.0	-30.0	1130.7 ms	-0.2	-22.0	-5.4	$C_{(2)}C_{(3)}$ str. + OCO wag
941.8 m	-1.8	-6.8	-4.8	-8.8	-7.0	-9.0	-15.8	937.7 w	-1.7	-6.0	-4.2	OCO sym. str. + CH_3 rock
897.4 s	-1.4	0.2	-2.2	-3.8	-0.2	-4.2	-4.0	913.5 vw	2.0	1.4	0.4	OH tor.
836.0 m	-7.0	0.0	0.0	-6.5	-1.1	-7.6	-7.6	842.0 ms	-7.9	-0.3	-0.9	CO_2^- sym. str. + CO_2^- o.p. bend
788.6 ms	-4.6	0.4	-4.9	-2.1	-0.5	-3.0	-2.6	794.5 w	-7.1	0.2	-4.4	CO_2^- o.p. bend + OCO wag
667.4 ms	-0.4	-3.4	-0.4	-13.4	-3.2	-13.2	-16.6	664.6 mw	-0.7	-3.9	-1.8	CO_2^- bend + OCO wag
463.4 ms	1.9	-0.8	4.8	0.4	0.0	1.2	0.4	-	-	-	-	OCO wag + CO_2^- bend + OCO bend
425.2 w	0.1	-0.2	-1.2	-6.6	-0.5	-6.9	-7.1	420.3 w	-0.2	0.0	-1.6	OCO bend
								269.4 mw	-0.4	-0.5	-4.9	CCC bend + $C_{(1)}C_{(2)}$ str.
A''												
3016.2 vs	-4.7	-9.4	-1.2	-3.3	-18.9	-12.8	-22.2	-	-	-	-	OH str.
2995.7 vw	0.3	0.3	-10.7	-0.2	-1.5	-2.0	-1.7	2992.0 ms	-0.3	-0.4	-10.4	CH_3 asym. str.
1602.6 vs	-43.6	-1.8	4.6	2.1	-0.2	3.7	1.9	1590.9 w	-36.7	0.0	2.0	CO_2^- antisym. str.
-	-	-	-	-	-	-	-	1455.1 m	-0.7	-1.4	-2.2	CH_3 asym.def.
1379.0 sh	1.0	-1.0	1.0	4.0	0.0	5.0	4.0	-	-	-	-	OH bend
1175.2 s	-0.5	-22.2	-2.2	-6.4	-22.2	-6.4	-28.6	1168.6 mw	-0.7	-25.7	-2.5	OCO antisym. str. + OCO rock + CH_3 rock
955.2 m	-1.2	-6.2	-5.2	-11.2	-7.1	-12.1	-18.3	952.9 w	-0.2	-5.6	-5.1	OCO antisym. str. + CH_3 rock
-	-	-	-	-	-	-	-	-	-	-	-	OH tor.
581.8 m	-1.8	-1.8	0.2	-10.9	-0.9	-10.0	-11.8	580.9 mw	-1.1	-0.6	0.6	OCO rock + CO_2^- rock
522.4 m	-0.4	-0.8	-3.4	-16.0	-0.8	-16.0	-16.8	532.4 w	-0.6	-1.4	-4.2	OCO twist
348.0 m								351.1 vvw	0.4	-3.1	0.4	CO_2^- rock + OCO twist

[a] Isotope shifts: $\Delta\nu_a$: $\nu_i(CH_3\text{-}C(OH)_2\text{-}{}^{13}CO_2^-) - \nu_i(CH_3\text{-}C(OH)_2\text{-}CO_2^-)$; $\Delta\nu_b$: $\nu_i(CH_3\text{-}{}^{13}C(OH)_2\text{-}CO_2^-) - \nu_i(CH_3\text{-}C(OH)_2\text{-}CO_2^-)$; $\Delta\nu_c$: $\nu_i({}^{13}CH_3\text{-}C(OH)_2\text{-}CO_2^-) - \nu_i(CH_3\text{-}C(OH)_2\text{-}CO_2^-)$; $\Delta\nu_d$: $\nu_i(CH_3\text{-}C({}^{18}OH)_2\text{-}CO_2^-) - \nu_i(CH_3\text{-}C(OH)_2\text{-}CO_2^-)$; $\Delta\nu_e$: $\nu_i(CH_3\text{-}{}^{13}C({}^{18}OH)_2\text{-}CO_2^-) - \nu_i(CH_3\text{-}C({}^{18}OH)_2\text{-}CO_2^-)$; $\Delta\nu_f$: $\nu_i(CH_3\text{-}{}^{13}C({}^{18}OH)_2\text{-}CO_2^-) - \nu_i(CH_3\text{-}{}^{13}C(OH)_2\text{-}CO_2^-)$; $\Delta\nu_g$: $\nu_i(CH_3\text{-}{}^{13}C({}^{18}OH)_2\text{-}CO_2^-) - \nu_i(CH_3\text{-}C(OH)_2\text{-}CO_2^-)$.

[b] Based on the potential energy distributions (P.E.D.), str.: stretch, def.: deformation, tor.: torsion, o.p.: out-of-plane.

Tables 1-4 give the observed frequencies of the four isotopic compounds and their assignments based on the potential energy distributions greater than 20% obtained in the normal coordinate calculation described in Section 3.5. The observed isotope shifts on ^{13}C- and ^{18}O-labelings in the CH_3 compounds are also listed in Tables 1 and 2. For the vibrational assignment we have assumed that this molecule takes the *gem*-diol form and has C_s symmetry, although it has an asymmetrical structure in the actual crystal [39]. Almost all the observed bands are interpreted on the basis of this structure. The normal vibrations are classified into the *A'* and *A"* species under this symmetry. Since this crystal has space group C_i^1 as described in Section 3.5, the crystal modes which are in out-of-phase and in-phase to a center of inversion are active in the IR and Raman spectra, respectively; therefore, many frequencies do not coincide with each other in the solid state spectra, some bands showing the large factor group splitting.

3.1. Vibrations of the OH groups

The broad and strong IR bands (multiplets) around 3000 (2250) cm^{-1} are attributed to the two OH (OD) stretching vibrations of the diol form. These bands are at lower frequencies than those of typical hydroxy compounds. Probably, this frequency lowering is attributed to coordination of the oxygen atom in one of the hydroxyl groups to the lithium atom and to intermolecular hydrogen bondings. A similar spectral feature is found for sodium fluoropyruvate hydrate existing in the diol form [23]. In metal complexes of ethylene glycol [43] a strong band due to the OH group coordinated to the metal ion occurs at 3170 cm^{-1}.

For Li-Pyr-H_2O the IR bands at 1539 and 1379 cm^{-1} are disappeared on O-deuteration; therefore, these bands are reasonably assigned to the OH bending vibrations (*A'* and *A"*). The corresponding bands in the CD_3 compound are at 1526 and 1376 cm^{-1}, respectively.

3.2. Vibrations of the CH_3 group

Whereas in the IR spectrum of Li-Pyr·H_2O the CH_3 asymmetric and symmetric stretching bands are obscured by the very strong OH bands in the 3000 cm^{-1} region, in the Raman spectrum the former bands strongly appear at 2992 and 2937 cm^{-1}. For Li-Pyr-d_3·H_2O the CD_3 stretching modes show strong Raman scattering at 2244 and 2125 cm^{-1}. The CH_3 asymmetric deformation bands (*A'* and *A"*) are overlapped by the COO^- symmetric stretching modes around 1420 cm^{-1} in the IR spectrum, but the corresponding Raman bands are clearly observed at 1455 cm^{-1}. Although their observed 3-^{13}C-shifts are slighter than expected, these shifts are reproduced well by the normal coordinate calculations (Supplementary data: Tables S1 and S2). The CH_3 symmetric deformation is easily assigned to the IR band at 1372 cm^{-1} and the Raman band at 1370 cm^{-1} from the large 3-^{13}C-shift. The order of the asymmetric and symmetric deformations (IR: 1029 and 1044 cm^{-1} and Raman: 1029 and 1057 cm^{-1}) is reversed in the CD_3 compounds from the results of the calculations. The CH_3 and CD_3 rocking vibrations are coupled with other vibrations to give complicated modes in the region of 1175-940 cm^{-1} and 835-625 cm^{-1}, respectively.

3.3. Vibrations of the COO^- group

The carboxylate group gives typical characteristic bands at 1603 and 1421 cm^{-1} as antisymmetric (*A"*) and symmetric (*A'*) stretching modes, respectively. These qualitative assignments are clearly confirmed by the 1-^{13}C-shifts as given in Table 1 and 2. However, the results of our normal vibration calculation indicate that the former is a localized vibration, whereas the latter is a vibration mixed complicatedly with other modes. Similar results were obtained for sodium pyruvate [24] and propionate [44].

Table 2. Observed frequencies, isotope shifts (cm^{-1}) [a], and assignments for solid Li-Pyr·D_2O.

IR	$\Delta\nu_{a'}$	$\Delta\nu_{b'}$	$\Delta\nu_{c'}$	Raman	$\Delta\nu_{a'}$	$\Delta\nu_{b'}$	$\Delta\nu_{c'}$	Assignments
A'								
2993.0 m	0.0	0.0	-10.5	2992.2 vs	-0.1	-0.3	-10.6	CH_3 asym. str.
2932.0 vw	9.0	7.3	-5.0	2934.0 vs	11.4	8.3	-4.7	CH_3 sym. str.
2284.8 vs	-1.6	-5.8	0.2	2268.5 w	1.0	-1.5	1.4	OD str.
1465.0 s	-11.0	-8.0	0.7	1478.9 s	-5.3	-5.9	-0.9	$C_{(1)}C_{(2)}$ str. + CH_3 asym.def + (CO_2^- sym. str.) [b]
1424.0 ms	-14.0	0.0	-2.0	1428.0 ms	-21.5	-1.9	-1.6	CH_3 asym.def.
1373.0 ms	-3.0	-1.0	-10.0	1369.8 vw	-1.8	-0.7	-9.9	CH_3 sym.def.
1266.0 ms	-2.7	-20.0	-3.8	1265.1 w	-2.4	-20.0	-2.9	OD bend + OCO wag
1145.5 s	-1.0	-24.3	-4.5	1142.6 w	-0.7	-23.7	-4.0	$C_{(2)}C_{(3)}$ str. + OCO sym. str.
-	-	-	-	1007.4 w	0.2	-2.6	-2.5	OD bend + $C_{(2)}C_{(3)}$ str. + CH_3 rock
947.0 w	-3.0	-6.0	-5.0	941.0 w	-3.3	-4.4	-5.3	OCO sym. str.+ CH_3 rock
848.0 ms	-8.0	0.0	-1.0	846.4 s	-8.3	-0.4	-1.1	CO_2^- o.p. bend + CO_2^- sym. str.
786.0 m	-19.0	0.0	-5.0	785.3 m	-18.8	-0.3	-5.2	CO_2^- o.p. bend + $C_{(1)}C_{(2)}$ str.
652.0 m	-0.7	0.0	0.0	-	-	-	-	OD tor. + OCO wag
637.0 m	-1.3	-4.0	-3.0	634.3 mw	-0.5	-3.8	-1.2	CO_2^- bend + OD tor.
462.0 m	-0.7	-2.0	0.5	-	-	-	-	OCO wag + CO_2^- bend
420.5 w	-1.5	-1.5	-2.5	413.8 w	0.0	-0.7	-2.5	OCO bend
				267.8 mw	0.0	-0.6	-4.9	CCC bend + $C_{(1)}C_{(2)}$ str.
A''								
2993.0 m	0.0	0.0	-10.5	2992.2 vs	-0.1	-0.3	-10.6	CH_3 asym. str.
2243.8 vs	-2.5	-18.6	-6.8	2241.5 m	-1.7	0.2	-2.9	OD str.
1606.0 vs	-44.3	-1.0	0.7	1596.8 m	-43.8	0.2	0.5	CO_2^- antisym. str.
1437.0 w	0.0	0.5	-2.3	1454.1 ms	-0.7	-0.8	-1.7	CH_3 asym.def.
1179.0 s	-1.5	-29.0	-3.0	1175.5 w	-0.8	-29.3	-3.3	OCO antisym. tr. + OCO rock + CH_3 rock
1020.0 s	-0.2	-1.8	-0.2	1017.1 sh	0.2	-1.0	0.6	OD bend + CH_3 rock
931.0 w	-1.0	-7.0	-4.0	930.8 w	0.0	-6.6	-3.4	OCO antisym. str. + CH_3 rock + OD bend
-	-	-	-	-	-	-	-	OD tor.
574.0 m	-2.0	-2.0	0.3	634.3 mw	-0.5	-3.8	-1.2	OCO rock + CO_2^- rock
514.0 sh	-1.0	-1.0	-3.0	519.5 w	-0.3	-0.2	-2.7	OCO twist
344.0 w				345.4 vvw	-1.4	0.2	-	CO_2^- rock + OCO twist

[a] Isotope shifts: $\Delta\nu_{a'}$: $\nu_i(CH_3\text{-}C(OD)_2\text{-}^{13}CO_2^-) - \nu_i(CH_3\text{-}C(OD)_2\text{-}CO_2^-)$; $\Delta\nu_{b'}$: $\nu_i(CH_3\text{-}^{13}C(OD)_2\text{-}CO_2^-) - \nu_i(CH_3\text{-}C(OD)_2\text{-}CO_2^-)$; $\Delta\nu_{c'}$: $\nu_i(^{13}CH_3\text{-}C(OD)_2\text{-}CO_2^-) - \nu_i(CH_3\text{-}C(OD)_2\text{-}CO_2^-)$.
[b] A small P.E.D. value (17%).

3.4. Skeletal vibrations

The 2-^{13}C and 2-C-^{18}O labelings shift many bands in the region below 1175 cm^{-1}. These bands are attributed to the CC and CO stretchings and the OCO deformations. However, the skeletal vibrations including these modes cannot be assigned straightforwardly as simple group vibrations, because these modes are complicatedly coupled. Their assignments have been made based on the potential energy distributions (P.E.D.).

3.5. Normal coordinate calculations

The structural parameters used in the calculation are based on our preliminary X-ray study [39]. However, the single crystals used in the analysis (triclinic, $P\bar{1}$ (C_i^1), a = 5.31(7) Å, b = 5.85(6) Å, c = 9.27(4) Å, α = 69(3)°, β = 68(3)°, γ = 62(2)°, Z = 2) were not good in quality for the precise analysis. The preparation of the good single crystals of this compound seems to be difficult, as suggested by Rach *et al.* [45]. Although no small values of R have been obtained, the structure is roughly as follows: the skeletal frame has C_s symmetry approximately, where the C-COO^- moiety is nearly planar and almost perpendicular to the C-C-C plane and bisected by the latter plane. The lithium cation forms an ionic bond to the carboxylate anion, while the oxygen atom in one of the *gem*-hydroxyl groups is coordinated to the cation. The OH bonds are not directed to the carboxylate group, judging from hydrogen bonds between the neighboring molecules. The bond lengths and angles are within the normal values except for the bonds around the lithium cation. This structure, including the conformation of the skeletal and the coordination of the cation, is almost the same as that in the crystals of sodium 3-fluoropyruvate hydrate which has the diol form [23], and both molecules are very similar in the bond lengths and angles.

On the other hand, Zhu *et al.* [34] reported a structure of the isolated molecule as a result of the quantum chemical calculation; it is different from that described above in the conformation around the C-CO_2 bond and in the directions of the O-H bonds. However, the former structure seems more probable from the viewpoint of the molecular structure in the crystalline state. For the vibrational calculations we used the model shown in Figure 5; the bond lengths and the bond angles are as follows: r($C_{(3)}$-H), 0.109 nm; r($C_{(2)}$-$C_{(3)}$), 0.152 nm; r($C_{(1)}$-$C_{(2)}$), 0.153 nm; r($C_{(1)}$-O), 0.1255 nm; r($C_{(2)}$-O), 0.1415 nm; r(O-H), 0.097 nm; CH_3 group, tetrahedral; δ($C_{(3)}$-$C_{(2)}$-O), 109.0°; δ($C_{(1)}$-$C_{(2)}$-O), 106.0°; δ(O-$C_{(2)}$-O), 111.0°; δ($C_{(1)}$-$C_{(2)}$-$C_{(3)}$), 115.7945°; δ($C_{(2)}$-O-H), 108.0°; δ($C_{(2)}$-$C_{(1)}$-O), 117.5°; and δ(O-$C_{(1)}$-O), 125.0°. Each of the O-H bonds is assumed to be in a position *trans* to the $C_{(2)}$-$C_{(1)}$ bond.

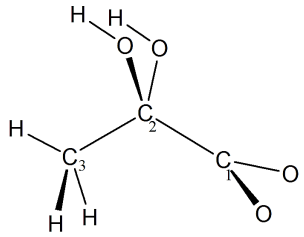

Figure 5. A molecular model having C_s symmetry.

We have carried out the normal vibration calculations according to the ***GF*** matrix method, using a Urey-Bradley force field to which some constants were added to obtain better agreement between the observed and calculated frequencies. In general, force field calculation by the least squares method gives reliable force constants [46]. Therefore, we have used this traditional method in the present study to obtain the refined force constants and then to accomplish the complete vibrational assignments for the pyruvate ion in the diol form and its isotopic compounds. The six internal coordinates, O'-$C_{(2)}$-O-H, O-$C_{(2)}$-O'-H', $C_{(1)}$-$C_{(2)}$-O-H, $C_{(1)}$-$C_{(2)}$-O'-H', $C_{(3)}$-$C_{(2)}$-O-H, and $C_{(3)}$-$C_{(2)}$-O'-H' (O'- H': the other hydroxyl group) were used for describing the two OH torsional modes. The torsional vibrations of the CH_3 and COO^- groups were excluded from the calculation.

Table 3. Observed frequencies (cm^{-1}) and assignments for solid Li-Pyr-d_3·H_2O.

IR	Raman	Assignments
A′		
2991.0 vs	2990.3 w	OH str.
2243.5 w	2244.3 s	CD_3 asym. str.
2126.0 vvw	2124.9 s	CD_3 sym.s tr.
1526.0 m	1519.8 w	OH bend + $C_{(1)}C_{(2)}$ str.
1417.0 s	1418.3 vs	CO_2^- sym. str.+ OH bend + CO_2^- bend
1127.0 s	1121.9 mw	$C_{(2)}C_{(3)}$ str. + CD_3 sym.def.
1105.0 s	1104.6 mw	OCO sym. str.
1044.0 ms	1056.8 m	CD_3 sym. def.
1029.0 m	1029.2 s	CD_3 asym. def.
895.0 s	-	OH tor.
838.0 sh	844.6 ms	CO_2^- sym. str.+ OCO sym. str.
779.0 m	778.0 vw	CO_2^- o.p. bend + CD_3 rock
740.0 w	733.5 m	CD_3 rock + CO_2^- bend + CO_2^- sym. str.
625.0 m	620.9 m	OCO wag + CD_3 rock + CO_2^- bend
457.0 ms	-	OCO wag + CO_2^- bend
405.0 w	395.2 w	OCO bend + OCO wag
	243.2 mw	CCC bend + $C_{(1)}C_{(2)}$ str.
A″		
2991.0 vs	2990.3 w	OH str.
2243.5 w	2244.3 s	CD_3 asym. str.
1601.0 vs	1591.3 w	CO_2^- antisym. str.
1376.0 s	1373.6 vw	OH bend
1181.3 s	1180.9 mw	OCO antisym. str. + OCO rock
1038.0 ms	1047.1 w	CD_3 asym.def.
-	-	OH tor.
834.0 ms	829.5 m	CD_3 rock
572.0 m	572.1 m	OCO rock + CO_2^- rock
508.0 m	516.2 mw	OCO twist + OCO rock
345.0 ms	349.0 vw	CO_2^- rock + OCO twist

Table 4. Observed frequencies (cm^{-1}) and assignments for solid Li-Pyr-d_3·D_2O.

IR	Raman	Assignments
A′		
2261.0 vs	2262.8 w	OD str.
-	2242.3 vs	CD_3 asym. str.
-	2138.7 ms	CD_3 sym. str.
1441.0 s	1437.7 ms	$C_{(1)}C_{(2)}$ str.+ CO_2^- sym. str.+ CO_2^- bend
1255.0 m	1256.0 w	OD bend + OCO wag
1114.0 s	1114.2 vw	$C_{(2)}C_{(3)}$ str.+ CD_3 sym. def.
1068.0 m	1063.0 sh	CD_3 sym. def.+ OCO sym. str.
1040.0 ms	-	CD_3 asym.def.
969.0 w	968.8 w	OD bend + CD_3 sym.def.+ OCO sym. str.
845.0 m	844.0 ms	CO_2^- sym. str.
791.0 w	792.4 w	CD_3 rock + CO_2^- o.p. bend
739.0 w	735.3 mw	CO_2^- bend + CO_2^- sym. str.
652.0 m	-	OD tor.
604.0 m	602.4 mw	CO_2^- bend
455.0 m	-	OCO wag + CO_2^- bend
390 sh	386.4 w	OCO bend + OCO wag
	242.6 mw	CCC bend + $C_{(1)}C_{(2)}$ str.
A″		
2261.0 vs	2262.8 w	OD str.
-	2242.3 vs	CD_3 asym. str.
1605.0 vs	1595.8 mw	CO_2^- antisym. str.
1182.0 s	1180.2 w	OCO antisym. str.+ OCO rock
-	1055.6 m	CD_3 asym. def.
1011.0 ms	1008.9 vw	OD bend
829.0 m	823.5 w	CD_3 rock + OCO antisym. str.
-	-	OD tor.
564.0 m	568.8 mw	OCO rock + CO_2^- rock
485.0 sh	479.5 w	OCO twist + OCO rock
-	343.9 vvw	CO_2^- rock + OCO twist

In the initial step the force constants were transferred from sodium acetate [46], *iso*-propanol [47] and so on and refined by the least-squares method. The final force constants give appreciably good agreement between the observed and the calculated frequencies for the normal and deuterated compounds except for a few frequencies. The ^{13}C- and ^{18}O-shifts are also reproduced well by these force constants. Some of discrepancies may come from the assumption that the molecule has C_s symmetry; exactly it is asymmetrical from the viewpoint of the whole molecule including the metal cation. The potential energy distributions (P.E.D.'s) indicate that the vibrations are very complicated except for the well-known group vibrations. The complete data, which includes the calculated frequencies, the calculated ^{13}C- and ^{18}O-shifts, P.E.D.'s, and the force constants, are given in Tables S1-S5 as the supplementary data. Thus, these results are consistent with the previous reports [3,4,6,7,33,34] that this molecule has the *gem*-diol structure in the solid state.

3.6. Relations among the isotope shifts

In Table 1, the observed 2-^{13}C-shifts ($\Delta\nu_b$) of Li-Pyr·H_2O (naturally abundant isotopic compound) are very similar to those ($\Delta\nu_e$) of its ^{18}O compound, and the observed ^{18}O-shifts ($\Delta\nu_d$) of Li-Pyr·H_2O to those ($\Delta\nu_f$) of its 2-^{13}C compound except for those of the 3016 cm^{-1} band. According to a perturbation treatment for small mass changes by Wilson *et al.* [48], the

characteristic values, λ_k ($=4\pi^2\nu_k^2$) for the perturbed (labeled) molecule, are expressed in terms of λ_k^0 and elements of the matrix consisting of $\boldsymbol{L}_0^{-1}$ for the unperturbed and $\Delta\boldsymbol{G}$ (the difference in the G matrixes between the perturbed and unperturbed species). $\Delta\boldsymbol{G}$ elements for each internal coordinate vary with mass differences of atoms to be labeled, as seen from the general formulas of $\boldsymbol{G}$ elements [46]. The difference in the $\boldsymbol{G}$ matrices between the 2-^{12}C(^{16}OH)$_2$ (A) and the 2-^{13}C(^{16}OH)$_2$ (B) compound is equal to that between the 2-^{12}C(^{18}OH)$_2$ (C) and the 2-^{13}C(^{18}OH)$_2$ (D) compound, and the difference between A and C to that between B and D. Consequently, $\Delta\nu_b$ should be approximately equal to $\Delta\nu_e$, and $\Delta\nu_d$ to $\Delta\nu_f$. The calculated shifts also indicate this relation clearly, as given in Table S1 (Supplementary data).

Furthermore, from the observed data in Table 1, we have found that these isotope shifts have the following additive property: $\Delta\nu_b + \Delta\nu_f = \Delta\nu_d + \Delta\nu_e = \Delta\nu_g$ (the shift from the 2-^{12}C(^{16}OH)$_2$ to the 2-^{13}C(^{18}OH)$_2$ compound). The calculated shifts also support the existence of the additivity as given in Table S1. In the same manner, we confirmed by the normal vibration calculation that there are such relations among the other stepwise-^{13}C-labeled isotopic compounds and the ^{12}C compound. Thus, it is possible to evaluate satisfactorily one set of the frequency shifts (e.g. $\Delta\nu_g$) from the other two sets of the observed shifts (e.g. $\Delta\nu_b$ and $\Delta\nu_d$).

4. Conclusions

In the present study almost all the observed IR and Raman bands of solid lithium pyruvate monohydrate and its isotopic compounds have been explained consistently in terms of the *gem*-diol structure, and a set of the reliable force constants which reproduce the observed frequencies has been obtained. In addition, it has been confirmed that the isotopic frequency shifts have the additive property among the ^{12}C, ^{13}C, ^{16}O, and ^{18}O compounds; such additivity is applicable to isotopic shifts of other compounds.

Acknowledgement

We wish to thank Ms. Yuriko Sugawa for her experimental assistance.

Supplementary material

Supplementary data (the calculated frequencies, the calculated isotope shifts, the P.E.D. values, and the force constants) associated with this article can be found in the online version.

References

[1]. Bayard, P. *Compt. Rend.* **1937**, *204*, 177-179.
[2]. Josien, M. L.; Joussot-Dubien, M.; Vizet, J. *Bull. Soc. Chim. Fr.* **1957**, 1148-1152.
[3]. Bellamy, L. J.; Willams, R. L. *Biochem. J.* **1958**, *68*, 81-84.
[4]. Anderson, D. M. W.; Bellamy, L. J.; Williams, R. L. *Spectrochim. Acta* **1958**, *12*, 233-238.
[5]. Jencks, W. P.; Carriuolo, J. *Nature* **1958**, *182*, 598-599.
[6]. Long, D. A.; George, W. O. *Trans. Faraday Soc.* **1960**, *56*, 1570-1581.
[7]. Long, D. A.; George, W. O. *Proc. Chem. Soc. London* **1960**, 242-243.
[8]. Gold, V.; Socrates, G.; Crampton, M. R. *J. Chem. Soc.* **1964**, 5888-5889.
[9]. Becker, M.; *Ber. Bunsenges.* **1964**, *68*, 669-676.
[10]. Greenzaid, P.; Luz, Z.; Samuel, D. *J. Am. Chem. Soc.* **1967**, *89*, 749-756.
[11]. Öjelund, G.; Wadsö, I. *Acta. Chem. Scand.* **1967**, *21*, 1408-1414.
[12]. Pocker, Y.; Meany, J. E.; Nist, B. J.; Zadorojny, C. *J. Phys. Chem.* **1969**, *73*, 2879-2882.
[13]. Larsen, P. O.; Wieczorkowska, E. *Acta. Chem. Scand.* **1974**, *B28*, 92-96.
[14]. Cooper, A. J. L.; Redfield, A. G. *J. Biol. Chem.* **1975**, *250*, 527-532.
[15]. Kokesh, F. C. *J. Org. Chem.* **1976**, *41*, 3593-3599.
[16]. Sciacovelli, O.; Dell'Atti, A.; De Giglio, A.; Cassidei, L. *Z. Naturforsch.* **1976**, *31c*, 5-11.
[17]. Cassidei, L.; Dell'Atti, A.; Sciacovelli, O. *Z. Naturforsch.* **1976**, *31c*, 641-645.
[18]. Cassidei, L.; Dell'Atti, A.; Sciacovelli, O. *Z. Naturforsch.* **1980**, *35c*, 1-5.
[19]. Hollenstein, H. *Ber. Bunsenges. Phys. Chem.* **1978**, *82*, 55-57.
[20]. Hollenstein, H.; Akermann, F.; Günthard, Hs. H. *Spectrochim. Acta* **1978**, *34A*, 1041-1063.
[21]. Katon, J. E.; Covington, D. T. *Spectrosc. Lett.* **1979**, *12*, 761-766.
[22]. Ray, W. J.; Katon, J. E.; Phillips, D. B. *J. Mol. Struct.* **1981**, *74*, 75-84.
[23]. Hurley, T. J.; Carrell, H. L.; Gupta, R. K.; Schwartz, J.; Glusker, J. P. *Arch. Biochem. Biophys.* **1979**, *193*, 478-486.
[24]. Kakihana, M.; Okamoto, M. *J. Phys. Chem.* **1984**, *88*, 1797-1804.
[25]. Fischer, G.; Flatau, S.; Schellenberger, A.; Zschunke, A. *J. Org. Chem.* **1988**, *53*, 214-216.
[26]. Rach, W.; Gattow, G. *Z. Anorg. Allg. Chem.* **1988**, *562*, 160-164.
[27]. Kivach, L. N.; Ksenofontov, M. A.; Podtynchenko, S. G.; Strekal, N. D. *Dokl. Akad. Nauk BSSR* **1989**, *33*, 321-324.
[28]. Hanai, K.; Kuwae, A.; Kawai, S.; Ono, Y. *J. Phys. Chem.* **1989**, *93*, 6013-6016.
[29]. Hanai, K.; Kawai, S.; Kuwae, A. *J. Mol. Struct.* **1991**, *245*, 21-27.
[30]. Kuwae, A.; Hanai, K.; Oyama, K.; Uchino, M. Lee, H.-H. *Spectrochim. Acta* **1993**, *49A*, 125-133.
[31]. Reva, I. D.; Stepanian, S. G.; Adamowicz, L.; Fausto, R. *J. Phys. Chem.* **2001**, A*105*, 4773-4780.
[32]. Duczmal, K.; Darowska, M.; Raczyńska, E. D. *Vib. Spectrosc.* **2005**, *37*, 77-82.
[33]. Hanai, K.; Kuwae, A.; Sugawa, Y.; Kunimoto, K.-K.; Maeda, S. *J. Mol. Struct.* **2007**, *837*, 101-106.
[34]. Zhu, J.; Geris, A. J.; Wu, G. *Phys. Chem. Chem. Phys.* **2009**, *11*, 6972-6980.
[35]. Nemenoff, R. A.; Snir, J.; Scheraga, H. A. *J. Phys. Chem.* **1978**, *82*, 2521-2526.
[36]. Murto, J.; Raaska, T.; Kunttu, H.; Räsänen, M. *J. Mol. Struct. (Theochem)* **1989**, *200*, 93-101.
[37]. Zhou, Z.; Du, D.; Fu, A. *Vib. Spectrosc.* **2000**, *23*, 181-186.
[38]. Duczmal, K.; Hallmann, M.; Raczyńska, E. D.; Gal, J.-F.; Maria, P.-C. *Polish J. Chem.* **2007**, *81*, 1011-1020.
[39]. Hanai, K.; Kuwae, A.; Kunimoto, K.-K.; Kitoh, S. (E-mail: hanai@nsc.nagoya-cu.ac.jp). Unpublished data.
[40]. Margolis, S. A.; Coxon, B. *Anal. Chem.* **1986**, *58*, 2504-2510.
[41]. Burton, T. M.; Degering, Ed. F. *J. Am. Chem. Soc.* **1940**, *62*, 227-227.
[42]. Tschelinzeff, W.; Schmidt, W. *Chem. Ber.* **1929**, *62*, 2210-2212.
[43]. Miyake, A. *Bull. Chem. Soc. Jpn.* **1959**, *32*, 1381-1383.
[44]. Kakihana, M.; Akiyama, M. *J. Phys. Chem.* **1987**, *91*, 4701-4709.
[45]. Rach, W.; Kiel, G.; Gattow, G. *Z. Anorg. Allg. Chem.* **1988**, *563*, 87-95.
[46]. Mizushima, S.; Shimanouchi, T. Sekigaisen Kyushu to Raman Koka (Infrared Absorptions and Raman Effects), Kyouritsu-Shuppan Co., Tokyo, 1970.
[47]. Tanaka, C. *Nippon Kagaku Zasshi* **1962**, *83*, 657-660.
[48]. Wilson, E. B. Jr; Decius, J. C.; Cross, P. C. Molecular Vibrations. The Theory of Infrared and Raman Vibrational Spectra, McGraw-Hill Book Co., Inc., New York, 1955.